GROUP ICA OF FUNCTIONAL MRI DATA: SEPARABILITY, STATIONARITY, AND INFERENCE

V. Calhoun[*§], T. Adali[§], G. Pearlson*[*], J. Pekar[†‡]*
*Division of Psychiatric Neuro-Imaging
and [†]Dept. of Radiology, Johns Hopkins University, Baltimore, MD 21205.
[‡]FM Kirby Research Center for Functional Brain Imaging,
Kennedy Krieger Institute, Baltimore, MD 21205.
[§]University of Maryland, Dept. of CSEE, Baltimore, MD 21250.

ABSTRACT

Independent component analysis (ICA) is being increasingly applied to functional MRI (fMRI) data. A principal advantage of this approach is its applicability to cognitive paradigms for which detailed *a priori* models of brain activity are not available. ICA has been successfully utilized to analyze single-subject fMRI data sets, and we have recently extended this work to provide for group inferences. In order to perform group analysis, we concatenate the single-subject images in time and perform a single ICA estimation, then back-reconstruct individual subject maps and time courses. When applied to fMRI data acquired during a simple visual paradigm, our group ICA analysis revealed task-related components in left and right visual cortex, a transiently task-related component in bilateral occipital/parietal cortex, and a non task-related component in bilateral visual association cortex. In this work, we develop three important areas needed for applying ICA to group data: separability, stationarity, and inference. Our results further demonstrate the utility of using such a method for making group inferences on fMRI data using ICA.

1. INTRODUCTION

Independent Component Analysis (ICA) is being increasingly applied to fMRI data [1,2]. ICA as applied to fMRI data can be used to separate either spatially [3] or temporally [4] independent sources and works well in both situations when appropriate assumptions are met [5,6]. We have recently developed an approach for performing an ICA analysis on a group of subjects [7,8]. This process is complicated by the different processing stages involved in the ICA analysis as well as the computational burden involved. For example, when using the general linear model, the investigator specifies the regressors of interest, and so drawing inferences about group data comes naturally, since all individuals in the group share the same regressors. In ICA, by contrast, different individuals in the group will have different time courses, and so it is not immediately clear how to draw inferences about group data using ICA. We present a model that facilitates the extension of ICA to group studies and discuss three important properties of such an analysis. First, group ICA relies upon the separability of the estimated mixing matrix across subjects. We discuss the implications of such a property and present simulation results demonstrating separability. Secondly, the ICA model we apply assumes stationary sources. While this is a reasonable assumption for some sources of interest, other sources are likely to be nonstationary. We discuss the implications of such a case and present simulation results demonstrating that the stationary sources can still be recovered. Finally, our method for making inference involves testing the amplitudes of the components maps across subjects. We discuss the important of scaling these maps by the norm of the time courses and compare these results with an analysis in which the ICA time courses are used in a regression analysis. In this work we focus on spatial ICA (i.e., calculation of spatially independent brain sources mixed by the hemodynamic response) although our methods can be applied to temporal ICA as well. We first review our Group ICA model.

2. THEORETICAL DEVELOPMENT

2.1 A group ICA model

We introduce the model in Figure 1 for discussion of group ICA. In the *data generation block* we assume that there is a set of statistically independent hemodynamic source locations in the brain (indicated by $s_i(v)$ at location v, a continuous number spanning the image space, for the i^{th} source). The sources

$$\mathbf{s}_p(v_p) = \left[s_1(v_p), s_2(v_p), ..., s_N(v_p) \right]^T \quad (1)$$

have weights that specify the contribution of each source to each voxel (at locations indicated by v_p, defined on $[0, D]$ for the p^{th} subject, where D is the size of the image); these weights are multiplied by each source's hemodynamic time course. Finally, it is assumed that each of the N sources are added together so that a given voxel contains a mixture of the sources, each of which fluctuates according to its weighted hemodynamic time course. This *linear mixing* is represented by the system, $\mathbf{A}$, and yields

$$\mathbf{u}_p(v_p) = \left[u_1(v_p), u_2(v_p), ..., u_N(v_p) \right]^T, \quad (2)$$

which represents N ideal samples of the signals $u_i(v)$ at location v, for the i^{th} source.

The first portion of the data generation block takes place within the brain. The second portion of the data generation block involves the fMRI scanner. We assume that K discrete time points were acquired with the scanner and that there are more time points acquired than there are sources in the brain. The sampling of the brain's hemodynamics with the fMRI scanner results in

$$\mathbf{y}_p(i_p) = \left[y_1(i_p), y_2(i_p), ..., y_K(i_p) \right]^T \quad (3)$$

where the fMRI data is discretely sampled in space (at locations indicated by $i_p = 1,2,...,V$ for the p^{th} subject, where V is the number of voxels).

The *post-processing block* is the primary concern of this work. The stages of analysis include a) preprocessing/spatial normalization, b) data reduction, c) estimation of independent components, and d) thresholding/presentation of the results. In the first stage (a), we have a transformation $\mathbf{T}(.)$ representing a number of possible preprocessing stages, including slice phase correction, motion correction, spatial normalization to a standard template brain [9], global scaling and smoothing. Following this stage, the effective spatial sampling for all subjects is indexed by $j = 1,2,...,M$, so that we now have

$$\mathbf{y}_p(j) = \left[y_1(j), y_2(j), ..., y_N(j) \right]^T \quad (4)$$

The second stage (b) consists of data reduction. Two reduction steps, one on data from each subject ($\hat{\mathbf{F}}_1^{-1} ... \hat{\mathbf{F}}_M^{-1}$) and one on an aggregate data set ($\hat{\mathbf{G}}^{-1}$), are used to reduce the computational load of simply entering all subjects' data into an ICA analysis prior to reduction. In the third stage (c), estimation of independent sources is performed. The fourth stage (d) involves grouping components across subjects and thresholding the resulting group ICA images.

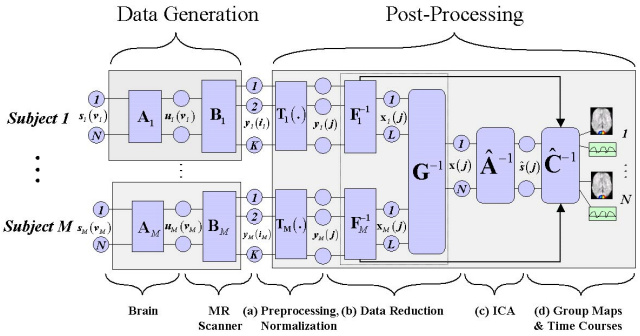

Figure 1: Model for Group ICA Analysis

To perform the group analysis, we make the assumption that the data collected from individual subjects are statistically independent observations. Thus $p_{xy}(x,y) = p_x(x)\, p_y(y)$ where $p_i(i)\big|_{i=x,y}$ is a probability density function (pdf) of a source from subject i and $p_{xy}(x,y)$ is the joint pdf for the same source for subjects x and y . Each subject is thus treated as an observation of the statistics of the population. Given this assumption, we will demonstrate that the unmixing matrix produced from the group ICA analysis will be largely separable across subjects.

2.2 Separability

We suggest entering all subjects into a single ICA analysis thus producing a single set of "group" components that can then be interpreted. The computational load of such an analysis can be decreased considerably by the incorporation of two data reduction stages as indicated. The data from the individual subjects are first reduced in dimension; these reduced data, from all subjects, are then concatenated in time. This data set is then further reduced resulting in a matrix that can be used in an ICA estimation stage.

The ICA maps from individual subjects are then back-reconstructed from the aggregate mixing matrix. A natural question which arises is how much the mixing coefficients associated with one subject are affected by the other subjects. Consider data in a voxel sampled at two time points from two subjects (subject x and subject y), $\mathbf{d}_x = [x_1\ x_2]$ and $\mathbf{d}_y = [y_1\ y_2]$, each of which is a normalized linear mixture of two hemodynamic sources. If we concatenate these subjects into a single vector, we have

$$\mathbf{d} = \left[\mathbf{d}_x \quad \mathbf{d}_y \right]^T \quad (5)$$

The data reduction and ICA analysis result in a mixing matrix

$$\mathbf{W} = \left[\begin{array}{cc|cc} \alpha_1 & \alpha_2 & \alpha_3 & \alpha_4 \\ \beta_1 & \beta_2 & \beta_3 & \beta_4 \end{array} \right] = \left[\mathbf{W}_x \quad \mathbf{W}_y \right] \quad (6)$$

and an estimate of the original sources $\hat{\mathbf{s}} = \mathbf{W}\mathbf{d}$ where $\mathbf{W}$ is partitioned to depict the submatrices corresponding to the original mixed sources. To back-reconstruct the individual subject maps we multiply the partition of $\mathbf{W}$ corresponding to the desired subject's data with the corresponding partition of $\mathbf{d}$ (e.g. $\mathbf{s}_x = \mathbf{W}_x \mathbf{d}_x$).

Since the goal of ICA is to yield independent components, the rows of $\hat{\mathbf{s}}$ will be approximately statistically independent. Additionally, data from each subject is expected to be independent of each other. Then, we write the expression for $\hat{\mathbf{s}}$

$$\hat{\mathbf{s}} = \left[\begin{array}{c} s_{11} + s_{12} \\ s_{21} + s_{22} \end{array} \right] \quad (7)$$

where we have defined $s_{11} = \alpha_1 x_1 + \alpha_2 x_2$, $s_{21} = \beta_1 x_1 + \beta_2 x_2$, $s_{12} = \alpha_3 y_1 + \alpha_4 y_2$, $s_{22} = \beta_3 y_1 + \beta_4 y_2$, and first note the statistical independence of s_{11} and s_{22} (and s_{12} and s_{21}). Since the ICA algorithm minimizes the dependence between the signals (rows of $\hat{\mathbf{s}}$), the dependence between s_{11} and s_{21} (and s_{12} and s_{22}) will be minimized by more heavily relying on the data within that subject, forcing the parameters for each subject to be primarily determined by that subject's observations. Thus, the individual unmixing matrices will be approximately separable across subjects (partitions) and the back-reconstructed data will be a function of primarily the data within subjects rather than across subjects.

We now consider the full model. Let $\mathbf{X}_i = \mathbf{F}_i^{-1}\mathbf{Y}_i$ be the $L - by - V$ reduced data matrix from subject i , where $\mathbf{Y}_i$ is the $K - by - V$ data matrix (containing the preprocessed and spatially normalized data), $\mathbf{F}_i^{-1}$ is the $L - by - K$ reducing matrix (determined by the PCA decomposition), V is the number of voxels, K is the number of fMRI time points and L is the size of the time dimension following reduction. Note that all inverses are considered to be psuedoinverses if the matrix is not square.

The next step is to concatenate the reduced data from all subjects into a matrix and reduce this matrix to N (the number of

components to be estimated). The $N-by-V$ reduced, concatenated matrix for the M subjects is

$$\mathbf{X}=\mathbf{G}^{-1}\begin{bmatrix}\mathbf{F}_1^{-1}\mathbf{Y}_1\\ \vdots \\ \mathbf{F}_M^{-1}\mathbf{Y}_M\end{bmatrix}. \quad (8)$$

where $\mathbf{G}^{-1}$ is an $N-by-LM$ reducing matrix (also determined by a PCA decomposition) and is multiplied on the right by the $LM-by-V$ concatenated data matrix for the M subjects.

2.2.1 ICA Estimation

Following ICA estimation, we can write $\mathbf{X}=\hat{\mathbf{A}}\hat{\mathbf{S}}$, where $\hat{\mathbf{A}}$ is the $N-by-N$ mixing matrix and $\hat{\mathbf{S}}$ is the $N-by-V$ component map. Substituting this expression for $\mathbf{X}$ into equation 8 and multiplying both sides by $\mathbf{G}$, we have

$$\mathbf{G}\hat{\mathbf{A}}\hat{\mathbf{S}}=\begin{bmatrix}\mathbf{F}_1^{-1}\mathbf{Y}_1\\ \vdots \\ \mathbf{F}_M^{-1}\mathbf{Y}_M\end{bmatrix}. \quad (9)$$

2.2.2 Partitioning

Partitioning the matrix $\mathbf{G}\hat{\mathbf{A}}$ by subject provides the following expression

$$\begin{bmatrix}\mathbf{G}_1\hat{\mathbf{A}}_1\\ \vdots \\ \mathbf{G}_M\hat{\mathbf{A}}_M\end{bmatrix}\hat{\mathbf{S}}=\begin{bmatrix}\mathbf{F}_1^{-1}\mathbf{Y}_1\\ \vdots \\ \mathbf{F}_M^{-1}\mathbf{Y}_M\end{bmatrix}. \quad (10)$$

We then write the equation for subject i by working only with the elements in partition i of the above matrices such that

$$\mathbf{G}_i\hat{\mathbf{A}}_i\hat{\mathbf{S}}_i=\mathbf{F}_i^{-1}\mathbf{Y}_i. \quad (11)$$

The matrix $\hat{\mathbf{S}}_i$ in equation 11 contains the single subject maps for subject i and is calculated from the following equation

$$\hat{\mathbf{S}}_i=\left(\mathbf{G}_i^{-1}\hat{\mathbf{A}}_i\right)^{-1}\mathbf{B}_i\mathbf{X}_i. \quad (12)$$

2.2.3 Single-subject maps and time courses

We now multiply both sides of equation 11 by $\mathbf{F}_i$ and write

$$\mathbf{Y}_i=\mathbf{F}_i\mathbf{G}_i\hat{\mathbf{A}}_i\hat{\mathbf{S}}_i, \quad (13)$$

which provides the ICA decomposition of the data from subject i, contained in the matrix $\mathbf{Y}_i$. The $N-by-V$ matrix $\hat{\mathbf{S}}_i$ contains the N source maps and the $K-by-N$ matrix $\mathbf{F}_i\mathbf{G}_i\hat{\mathbf{A}}_i$ is the single subject mixing matrix and contains the time course for each of the N components.

2.3 Stationarity

We have assumed throughout that the sources are stationary; that is their distributions do not change with time (or across subjects). It is reasonable to assume that the signals of interests (e.g. activation due to a specific task or of a specific brain network) will be largely stationary (this is the basic motivation for group inference in the first place). In practice, this is not the case for *subject specific* signals such as motion or physiologic noise. That is, there are non-stationary signals present in the data as well. But, how do the presence of non-stationary signals affect the group analysis? Consider two sources again, one containing stationary brain activation and one having a subject specific distribution. Assuming independence of the sources, the estimated source distributions may be written as:

$$\hat{p}(\mathbf{s};i)=\begin{cases}\hat{p}(s_1)\hat{p}_i(s_2) & i=x\\ \hat{p}(s_1)\hat{p}_i(s_2) & i=y\end{cases} \quad (14)$$

where $\hat{p}(\mathbf{s};i)$ is the pdf for subject i, $\hat{p}(s_1)$ is the estimated pdf for source 1 and $\hat{p}_i(s_2)$ is the estimated pdf for source 2. Using a stationary source model, it is not possible to estimate the nonstationary source distributions correctly. However the source s_1 can still be estimated. This can be seen by writing the histogram estimated source pdf:

$$\hat{p}(\mathbf{s})=\hat{p}(s_1)\sum_{i=1}^{M}\frac{1}{M}\hat{p}_i(s_2), \quad (15)$$

The time varying portion of the source pdf is collapsed across time and the resulting individual source distributions are based upon the entire data. Thus we are able to estimate s_1, but the other source will have a distribution that is averaged across subjects. This is not a physiologically meaningful source and can be considered noise. It is useful to consider that some of the sources that are difficult to interpret in ICA of fMRI data may be due to nonstationary sources. This result will also be demonstrated in a simulation.

2.4 Inference

Thresholding the resulting group ICA maps using a Z-threshold criterion as suggested for single subject analysis [3] provides information about which regions are contributing significantly to an individual component map. In a group study, we are interested in which components are *consistently* contributing significantly. We thus suggest reconstructing single subject ICA maps from the group ICA estimation and calculating the mean and variance of each component across subjects, where the variance across subjects is used as an estimate of the *population* variance [10]. A hypothesis test can then be used to provide a "random effects" inference: the magnitudes or weights of the voxels within a set of ICA components are treated as random variables and a one-sample t-test with the null hypothesis of zero magnitude is performed. This is related to general linear model approaches in which the estimated amplitudes are tested for a significant difference from zero [11]. As the ICA analysis produces estimates of hemodynamic sources, there is a physiologic meaning to the results and such an approach is justified.

Two important points involve normalization. First, we recommend as a preprocessing stage scaling the data across subjects to the same global mean. The scaling is a function of the gain used for the scan acquisition and typically varies between scan sessions. Normalizing by the global mean prevents subjects scanned with high gains from dominating the analysis. Second, the back-reconstructed component maps should be multiplied by the standard deviation of the mixing matrix prior to the

hypothesis test. In most ICA estimation approaches, the components are forced to have a standard deviation of 1 and the amplitude of the time courses is allowed to vary. As the MRI signal strength is the measure of interest, it is desirable to normalize the amplitude of the time courses when performing inference. This also parallels a regression analysis, in which the regressor is normalized and the estimated amplitude is a relative measure of the MRI signal strength. This approach provides a measure of the amplitude in terms of MRI signal, whereas the independent component amplitude is potentially confounded with the amplitude of the time course.

3. EXPERIMENTS AND METHODS

3.1 Simulated Experiment: Separability

A simulation was performed to determine how the sources that were back-reconstructed from the aggregate mixing matrix would compare with sources that were generated from an ICA analysis performed separated on each "subject". In order to determine this matrix, we simulated nine "subjects". Eight of the nine subjects only had one source embedded within the data. The ninth subject had two sources (similar to the sources in the previous simulation). $30-by-30$ spatial "sources" and associated 80-point hemodynamic mixing time courses were generated for each subject. Each source was flattened into a 900-element vector and the two subsequently mixed by the hemodynamic time courses, resulting in a $900-by-80$ matrix. Zero mean, Gaussian noise was then added to the mixed sources such that the contrast-to-noise ratio (CNR) for the largest simulated fMRI "activation" was 3.9, slightly less than half the CNR for our fMRI experiment. Each individual "subject" was first reduced from 80 time points to 20 time points using PCA and the resulting data sets were concatenated together into an aggregate data set, resulting in a $900-by-180$ matrix. The number of sources was then further reduced using PCA to 2, followed by independent component estimation. This yielded a set of aggregate components and time courses. The individual time courses and maps were then reconstructed and thresholded as described earlier. Additionally, we performed an ICA analysis on each subject individually and generated subjects' maps for comparison with the back-reconstructed maps.

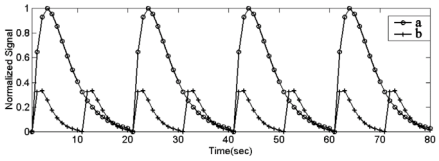

Figure 2: Mixing matrix used for simulation

3.2 Simulated Experiment: Stationarity

We designed a simulation to evaluate the effect of nonstationary sources upon the ICA estimation. We generated a data set containing eight simulated subjects with two sources present. One sources was stationary across subjects and the other source was stationary within subjects, but varied across subjects. An eighty element mixing matrix for each source and each subject was generated and used to mix the data. The data were concatenated in time and reduced to eight time points, concatenated in time, and reduced to two time points followed by an ICA unmixing.

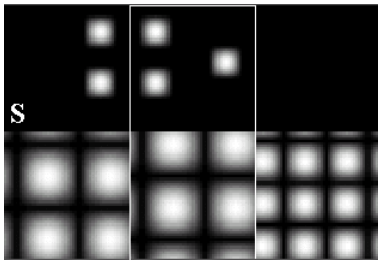

Figure 3: Stationary source (S) and five sources which change from subject to subject.

3.3 fMRI Experiment

The Johns Hopkins Institutional Review Board approved the protocol and all participants provided informed consent. Data from nine normal subjects were acquired on a Philips 1.5T Scanner. Functional scans were acquired with an echo planar sequence (64x64, flip angle=90, TR=1s, TE=39ms) over a 6-minute period for a total of 360 time points. Nine slices were acquired, centered on the occipital pole and the frontal pole. A visual paradigm was presented in which an 8Hz reversing black and white checkerboard was presented intermittently in the left and right visual fields for thirty seconds at a time.

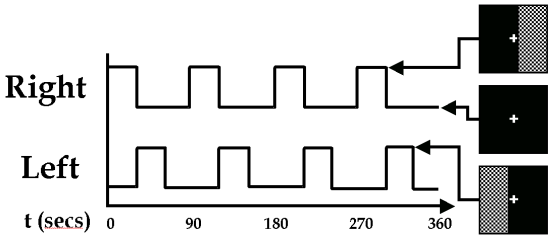

Figure 4: Paradigm for fMRI experiment

Preprocessing: The images were first corrected for timing differences between the slices using windowed Fourier interpolation to minimize the dependence upon which reference slice is used [12,13]. Next, the data were imported into the Statistical Parametric Mapping software package, SPM99 [14]. Data were motion corrected, spatially smoothed with a 6x6x10 mm Gaussian kernel, and spatially normalized into the standard space of Talairach and Tournoux [9]. The data were slightly subsampled to 3x3x4mm, resulting in 53x63x34 voxels. For display here, slices ten through twenty-five were presented.

ICA: An AIC/MDL estimation on two subjects was performed which predicted in both subjects *fewer* than 40 sources. Data from each subject were reduced from 360 time points to 40 time points using PCA. The results are not very sensitive to the reduction parameter, however the original data should not be overly reduced to avoid losing important information. Data from all subjects were then concatenated and this aggregate data set was entered into an AIC/MDL estimation to determine the

number of sources existing in the group data. The aggregate data were then reduced to this dimension using PCA, followed by an independent component estimation using an algorithm which attempts to minimize mutual information [1]. Time courses and spatial maps were then reconstructed for each subject and the spatial maps were thresholded at $p < 0.001$ ($t = 4.5$, $df = 8$).

4. RESULTS

Results from simulation 1 are presented in Figure 5. ICA spatial maps generated from individual subjects were very similar to spatial maps back-reconstructed from the aggregate mixing matrix.

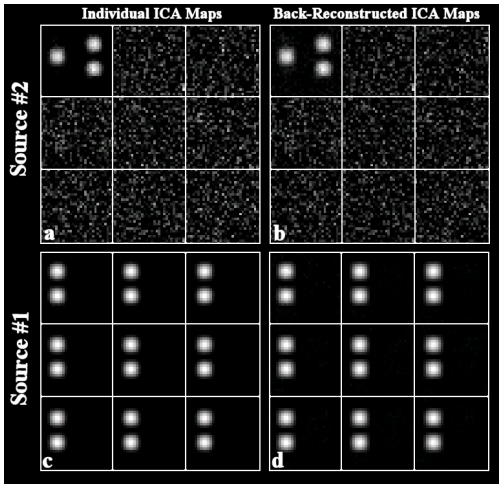

Figure 5: Comparison of individual ICA maps for nine simulated subjects with back-reconstructed ICA maps

Results from simulation 2 are presented in Figure 6. The stationary source estimate was remarkably good. The non stationary sources were all captured in the same component and represented a time averaged source distribution.

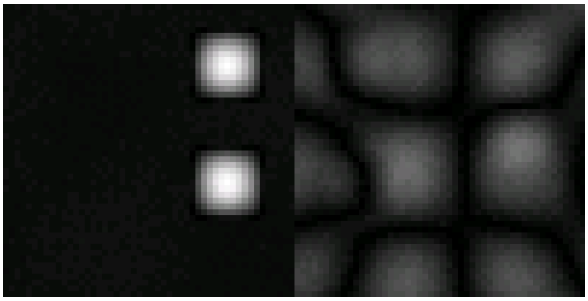

Figure 6: Estimated sources for data containing stationary (left) and non stationary (right) sources.

Group maps for the fMRI ICA analyses are presented in Figure 7. The number of components was estimated to be twenty-one by both MDL and AIC so the aggregate data were reduced to this dimension and twenty-one components were estimated. Both maps are thresholded at $p < 0.001$ ($t = 4.5$, $df = 8$). There were several interesting components within the data. Separate components for primary visual areas on the left and the right visual cortex (depicted in red and blue, respectively) were consistently task-related with respect to the appropriate stimulus. A large region (depicted in green) including occipital areas and extending into parietal areas appeared to be sensitive to changes in the visual stimuli. Additionally we identified visual association areas (depicted in white) that were consistently detected across the group of subjects, however the time courses were not task related.

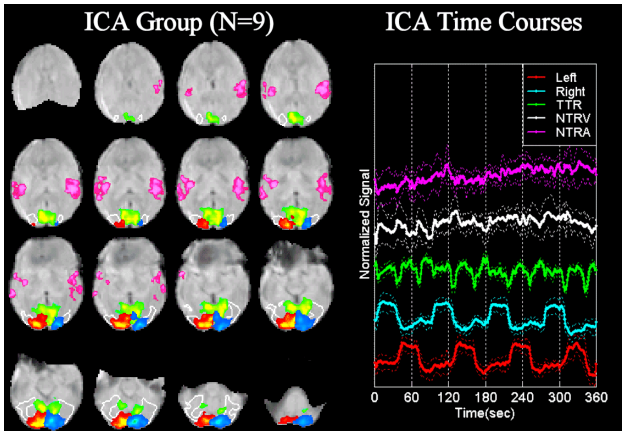

Figure 7: fMRI Group ICA results

5. SUMMARY

We have presented a method for making group inference maps through the application of independent component analysis to fMRI data. We have applied it to a simple visual paradigm and identified several distinct visual areas which were either consistently task-related, transiently task-related, or correlated but non task-related.

Starting from the assumption that data from subjects represent independent observations, we have demonstrated that the aggregate mixing matrix is separable across subjects. We have also demonstrated that group ICA of fMRI data can be used to estimate sources of interest even when other sources (such as motion or other artifacts) are not stationary. Fortunately, most fMRI sources of interest are largely stationary across subjects due to the fMRI paradigm design.

The most powerful aspect of group ICA lies in the ability to make inferences about a group of subjects. The application of a preprocessing stage in which the global average for each subjects' data is normalized to the same value as well as normalization of the back-reconstructed spatial maps by the time course variance is emphasized.

In conclusion, we have extended independent component analysis of fMRI data to provide for group inferences. Our method has general applicability, is straightforward to apply, and should be computationally reasonable for many fMRI group studies.

6. REFERENCES

[1] A.J.Bell and T.J.Sejnowski, An Information Maximisation Approach to Blind Separation and Blind Deconvolution *Neural Computation*, vol. 7, pp. 1129-1159, 1995.

[2] M.J.McKeown, S.Makeig, G.G.Brown, T.P.Jung, S.S.Kindermann, A.J.Bell, and T.J.Sejnowski, Analysis of FMRI Data by Blind Separation Into Independent Spatial Components *Hum.Brain Map.*, vol. 6, pp. 160-188, 1998.

[3] M.J.McKeown, T.P.Jung, S.Makeig, G.Brown, S.S.Kindermann, T.W.Lee, and T.J.Sejnowski, Spatially Independent Activity Patterns in Functional MRI Data During the Stroop Color-Naming Task *Proc Natl Acad Sci*, vol. 95, pp. 803-810, 1998.

[4] B.B.Biswal and J.L.Ulmer, Blind Source Separation of Multiple Signal Sources of FMRI Data Sets Using Independent Component Analysis *J.Comput.Assist.Tomogr.*, vol. 23, pp. 265-271, 1999.

[5] M.J.McKeown and T.J.Sejnowski, Independent Component Analysis of FMRI Data: Examining the Assumptions *Hum.Brain Map.*, vol. 6, pp. 368-372, 1998.

[6] V.D.Calhoun, T.Adali, G.D.Pearlson, and J.J.Pekar, Spatial and Temporal Independent Component Analysis of Functional MRI Data Containing a Pair of Task-Related Waveforms *Hum Brain Mapp.*, vol. 13, pp. 43-53, 2001.

[7] V.Calhoun, T.Adali, G.Pearlson, and J.Pekar, A Method for Making Group Inferences Using Independent Component Analysis of Functional MRI Data: Exploring the Visual System *Neuroimage*, vol. 13, no. 6, p. S88, 2001.

[8] V.Calhoun, T.Adali, G.Pearlson, and J.Pekar, A Method for Making Group Inferences From Functional MRI Data Using Independent Component Analysis *Hum.Brain Map.*, vol. 14, 2001.

[9] J.Talairach and P.Tournoux, *A Co-Planar Sterotaxic Atlas of a Human Brain*, Thieme, Stuttgart: 1988.

[10] R.P.Woods, Modeling for Intergroup Comparisons of Imaging Data *Neuroimage.*, vol. 4, p. S84-S94, 1996.

[11] A.P.Holmes and K.J.Friston, Generalizability, Random Effects, and Population Inference *Neuroimage.*, vol. 7, p. S754, 1998.

[12] P.F.van de Moortele, B.Cerf, E.Lobel, A.L.Paradis, A.Faurion, and D.Le Bihan, Latencies in FMRI Time-Series: Effect of Slice Acquisition Order and Perception *NMR Biomed.*, vol. 10, pp. 230-236, 1997.

[13] V.Calhoun, X.Golay, and G.Pearlson, Improved fMRI Slice Timing Correction: Interpolation Errors and Wrap Around Effects *Proceedings, ISMRM, 9th Annual Meeting, Denver*, p. 810, 2000.

[14] K.J.Worsley and K.J.Friston, Analysis of FMRI Time-Series Revisited--Again *Neuroimage.*, vol. 2, pp. 173-181, 1995.